7. *Theory of Eden's Twin Strips and Application of It to Magnifying Mechanism of Seismometer.*

By Genrokuro NISHIMURA, Masazi SUZUKI,

Earthquake Research Institute,

and Eiichi FURUKAWA,

Faculty of Engineering, Chuo University, Tokyo.

(Read Oct. 21, 1949 and Sept. 16, 1953.—Received Jan. 8, 1954.)

1. Introduction.

A simple and ingenious magnifying mechanism, known as "Eden's twin strips", has been used chiefly for comparators of high sensitivity such as the Millionth Comparator. So far as we know, it has not been used for the measurements of vibration. However, it is a matter of practical interest to find useful applications to such purpose because of its outstanding advantages which include freedom from backlash and solid friction, high magnification and simple construction. After some preliminary investigations, it was found to be available for such purpose to the best advantage. Hitherto we have found a broad application in the field of the vibration-measuring instruments such as a vibrograph[1], an accelerograph[2], a torsiograph[3], a vibration table[4], and a penmotor[5] and others[6]. It has given satisfactory service in a considerable variety of applications over a period of about five years, and

1) The example is shown in the present paper.

2) G. NISHIMURA, M. SUZUKI & S. KAWAHARA, "Vibration of Machine-Tool.: Horizontal vibration of Grinder," *Soc. Precision Mechanics, Japan*, **18**, No. 10, (1952). G. NISHIMURA & H. KAWASUMI, "Torsional Moment of a Focal Plane Shutter Camera," *Jour. Fac. Eng., Univ. Tokyo*. **24**, No. 2, (1954).

3) G. NISHIMURA & E. FURUKAWA, "Torsiograph and its Application," read on Spring League Meeting of the Soc. of Machine Engineering & the Soc. of Precision Mechanics, Feb. 10, (1951).

G. NISHIMURA & others, "A New-Designed Prospecting Apparatus," *Bull. E.R.I.*, **31**, No. 4, (1954).

4) G. NISHIMURA, M. SUZUKI & S. KAWAHARA, "Measurement of the Reactional Force of Sewing Machine," *Soc. Precision Mechanics, Japan*, **18**, No. 6, (1952).

5) K. KANAI & T. TANAKA, "A Smoked-paper Recorder for High Sensitive Seismometer," *Zisin*, [ii], **5**, No. 3, (1953).

6) G. NISHIMURA & E. FURUKAWA, "Dynamical Measurement of Mesh Error of Gear Trains in Working Condition," read on Spring League Meeting of the Soc. of Mech. Engineering and the Soc. of Precision Mechanics, Feb. 10, (1951).

this fact has encouraged the writers in preparing this paper.

The present paper describes its statical and dynamical characteristics which is determined theoretically and confirmed by the experiments using a vibration table, and furnishes sufficient informations for purposes of designing.

2. Statical Characteristics.

In Fig. 1, suppose that the twin strips are in equilibrium under the action of the known external forces P_0, Q_0 and couple M_0, and the member B_1B_2 is massless and absolutely rigid. Then, the resultant of all external forces acting on a recording pen (or a deflecting mirror) can be completely defined by P_0, Q_0 and M_0. Let P, Q and M denote the longitudinal force (restoring force of the twin strips), the shearing force, and the bending moment at the clamped end A_1, respectively. The signs of these quantities are defined as positive as shown in Fig. 1. Let EI_s denote the flexural rigidity of strips, δ the displacement of the clamped end A_1 from its equilibrium position, θ the slope of strips at the end B_2 ($x_2=l$), Y the deflection at the same point, and l and D the length of strips and the distance between both strips, respectively.

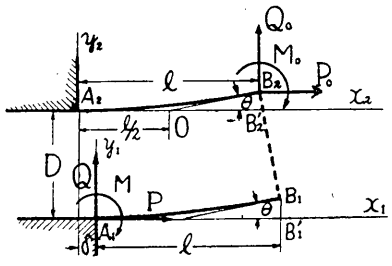

Fig. 1.

Taking coordinate axes, as shown in Fig. 1, and denoting

$$P'=P+P_0\,,\quad Q'=Q+Q_0\,,\quad M'=M+M_0\,,$$

the differential equations for deflection curve of strips may be written in the form

$$\frac{d^2y_1}{dx_1^2}+\frac{P}{EI_s}y_1=\frac{Q}{EI_s}x_1+\frac{M}{EI_s}\,,$$

$$\frac{d^2y_2}{dx_2^2}-\frac{P'}{EI_s}y_2=-\frac{Q'}{EI_s}x_2-\frac{M''}{EI_s}\,,$$

and

$$M''=M'-PD+P_0Y-Q\delta-Q_0l\,.$$

The solutions of these equations satisfying the conditions at the clamped ends are

$$y_1=-\frac{M}{P}\cos\sqrt{\frac{P}{EI_s}}\,x_1-\frac{Q}{P}\sqrt{\frac{EI_s}{P}}\sin\sqrt{\frac{P}{EI_s}}\,x_1+\frac{Q}{P}\,x_1+\frac{M}{P}\,,$$

$$y_2=-\frac{M''}{P'}\cosh\sqrt{\frac{P'}{EI_s}}\,x_2-\frac{Q'}{P'}\sqrt{\frac{EI_s}{P'}}\sinh\sqrt{\frac{P'}{EI_s}}\,x_2+\frac{Q'}{P'}\,x_2-\frac{M''}{P'}\ ,$$

which, for small values of $\sqrt{\frac{P}{EI_s}}\,x_1$, and $\sqrt{\frac{P'}{EI_s}}\,x_2$, become

$$y_1=\frac{M}{EI_s}\frac{x_1^2}{2}\left\{1-\frac{1}{12}\left(\frac{P}{EI_s}\right)x_1^2+\frac{1}{360}\left(\frac{P}{EI_s}\right)^2x_1^4-\cdots\right\}$$
$$+\frac{Q}{EI_s}\frac{x_1^3}{6}\left\{1-\frac{1}{20}\left(\frac{P}{EI_s}\right)x_1^2+\frac{1}{840}\left(\frac{P}{EI_s}\right)^2x_1^4-\cdots\right\},\quad\cdots\cdots\cdots(1.1)$$

$$y_2=-\frac{M''}{EI_s}\frac{x_1^2}{2}\left\{1+\frac{1}{12}\left(\frac{P'}{EI_s}\right)x_2^2+\frac{1}{360}\left(\frac{P'}{EI_s}\right)^2x_2^4+\cdots\right\}$$
$$-\frac{Q}{EI_s}\frac{x_2^3}{6}\left\{1+\frac{1}{20}\left(\frac{P'}{EI_s}\right)x_2^2+\frac{1}{840}\left(\frac{P'}{EI_s}\right)^2x_2^4+\cdots\right\}.\quad\cdots\cdots\cdots(1.2)$$

Case (1) $P_0=Q_0=M_0=0$:

Let us begin with a discussion of some particular case in which the problem is simplified. If we put $P_0=Q_0=M_0=0$, i.e., if there are no external forces and couples, the expressions (1.1), (1.2) can be reduced to

$$y_1=\frac{M}{EI_s}\frac{x_1^2}{2}\left\{1-\frac{1}{12}\left(\frac{P}{EI_s}\right)x_1^2+\cdots\right\}$$
$$+\frac{Q}{EI_s}\frac{x_1^3}{6}\left\{1-\frac{1}{20}\left(\frac{P}{EI_s}\right)x_1^2+\cdots\right\},\quad\cdots\cdots\cdots(1.3)$$

$$y_2=\frac{1}{EI_s}\frac{x_2^2}{2}(-M+PD+Q\delta)\left\{1+\frac{1}{12}\left(\frac{P}{EI_s}\right)x_1^2+\cdots\right\}$$
$$-\frac{Q}{EI_s}\frac{x_2^2}{6}\left\{1+\frac{1}{20}\left(\frac{P}{EI_s}\right)x_2^2+\cdots\right\}.\qquad\cdots\cdots\cdots(1.4)$$

First, keeping only the first term in the expansion, we can readily obtain the following approximate expressions:

$$\left.\begin{aligned}P&=\frac{2EI_s}{lD}\cdot\theta\cdot\left\{1+\frac{3}{2}\left(\frac{D}{l}\right)^2\theta^2\right\},\\ Q&=-\frac{2EI_s}{lD}\cdot\frac{3}{2}\left(\frac{D}{l}\right)^2\cdot\theta^2,\\ M&=\frac{EI_s}{l}\cdot\theta\left\{1+\frac{3}{2}\left(\frac{D}{l}\right)\theta\right\}.\end{aligned}\right\}\qquad\cdots\cdots\cdots(1.5)$$

Next, keeping the first two terms in the expansion, the expressions (1.3), (1.4) become

$$y_1=\frac{M}{EI_s}\cdot\frac{x_1^2}{2}\left\{1-\frac{1}{12}\left(\frac{P}{EI_s}\right)x_1^2\right\}+\frac{Q}{EI_s}\cdot\frac{x_1^3}{6}\left\{1-\frac{1}{20}\left(\frac{P}{EI_s}\right)x_1^2\right\}, \qquad \cdots\cdots(1.6)$$

$$y_2=\frac{1}{EI_s}\cdot\frac{x_2^2}{2}(-M+PD+Q\delta)\left\{1+\frac{1}{12}\left(\frac{P}{EI_s}\right)x_2^2\right\} -\frac{Q}{EI_s}\cdot\frac{x_2^3}{6}\left\{1+\frac{1}{20}\left(\frac{P}{EI_s}\right)x_2^2\right\}. \qquad \cdots\cdots(1.7)$$

The geometrical relationship at $x_1=x_2=l$

$$\left(\frac{dy_1}{dx_1}\right)=\left(\frac{dy_2}{dx_2}\right)=\tan\theta\approx\theta \qquad \cdots\cdots(1.8)$$

gives

$$\frac{M}{EI_s}l-\frac{PM}{(EI_s)^2}\cdot\frac{l^3}{6}+\frac{Q}{EI_s}\cdot\frac{l^2}{2}-\frac{PQ}{(EI_s)^2}\cdot\frac{l^4}{24}=\theta,$$

$$\frac{l}{EI_s}(-M+PD+Q\delta)+\frac{P}{(EI_s)^2}\cdot\frac{l^3}{6}(-M+PD+Q\delta) -\frac{Q}{EI_s}\cdot\frac{l^2}{2}-\frac{PQ}{(EI_s)^2}\cdot\frac{l^4}{24}=\theta,$$

from which we obtain

$$Q=\frac{EI_s}{l}\cdot\frac{\left\{2\theta-\frac{PlD}{EI_s}+\frac{P^3D}{(EI_s)^3}\cdot\frac{l^5}{36}\right\}}{\left\{\delta+\frac{P}{EI_s}\cdot\frac{l^3}{12}-\frac{P^2\delta}{(EI_s)^2}\cdot\frac{l^4}{36}\right\}}, \qquad \cdots\cdots(1.9)$$

$$M=\frac{EI_s}{l}\cdot\frac{\left\{-l\theta+\delta\theta+\frac{Pl^2D}{2EI_s}+\frac{Pl^2\delta\theta}{6EI_s}+\frac{P^2l^4D}{24(EI_s)^2}-\frac{P^3l^6D}{144(EI_s)^2}\right\}}{\left\{\delta+\frac{P}{EI_s}\cdot\frac{l^3}{12}-\frac{P^2\delta}{(EI_s)^2}\cdot\frac{l^4}{36}\right\}} \qquad \cdots\cdots(1.10)$$

From the geometrical considerations, we con see that

$$\delta+\overline{A_1B_1'}=D\sin\theta+\overline{A_2B_2'},$$

or

$$\delta\approx D\theta, \qquad \cdots\cdots(1.11)$$

and

$$y_{1_{x_1=l}}+D\cos\theta=D+Y\,,$$

or

$$y_{1_{x_1=l}}-Y\approx\frac{D}{2}\theta^2\,. \qquad \ldots\ldots\ldots(1.12)$$

From the expressions (1.6), (1.7) and (1.8), we obtain

$$\frac{M}{EI_s}l^2+\frac{Q}{EI_s}\cdot\frac{l^3}{3}-\frac{Pl^2D}{2EI_s}-\frac{Ql^2\delta}{2EI_s}-\frac{P^2l^4D}{24(EI_s)^2}-\frac{PQl^4\delta}{24(EI_s)^2}=\frac{D}{2}\theta^2.$$

$\ldots\ldots\ldots(1.13)$

Introducing the expressions (1.9), (1.10) into Eq. (1.13) and using the expression (1.11), we obtain the equation from which the restoring force P has to be determined. Thus

$$f(P)=-\frac{l^7D}{864(EI_s)^3}\cdot P^3+\frac{l^4D^2\theta^3}{72(EI_s)^2}\cdot P^2+\frac{l^3D}{6EI_s}\cdot P-\frac{D^2}{2}\cdot\theta^3-\frac{l^2}{3}\theta=0\,.$$

Let the approximate solution of $f(P)=0$ be $\left(\frac{2EI_s}{lD}\theta+u\right)$, in which we know that u is small. Therefore the equation $f(P)=0$ becomes, on neglecting powers of u beyond the first,

$$f\left(\frac{2EI_s}{lD}\theta\right)+uf'\left(\frac{2EI_s}{lD}\theta\right)=0\,,$$

whence an approximate value of u is

$$u=-\frac{f\left(\frac{2EI_s}{lD}\theta\right)}{f'\left(\frac{2EI_s}{lD}\theta\right)}=\frac{2EI_s}{lD}\cdot\theta\cdot\frac{\left\{\frac{3}{2}\left(\frac{D}{l}\right)^2\theta^2+\frac{1}{36}\left(\frac{l}{D}\right)^2\theta^2\right\}}{\left\{1-\frac{1}{12}\left(\frac{l}{D}\right)^2\theta^2\right\}}\,.$$

Consequently, the approximate expression for P becomes

$$P=\frac{2EI_s}{lD}\cdot\theta\cdot\left[1+\frac{\left\{\frac{3}{2}\left(\frac{D}{l}\right)^2+\frac{1}{36}\left(\frac{l}{D}\right)^2\right\}}{\left\{1-\frac{1}{12}\left(\frac{l}{D}\right)^2\theta^2\right\}}\cdot\theta^2\right]=\frac{2EI_s}{lD}\theta\cdot(1+\alpha\theta^2)\,,$$

$\ldots\ldots\ldots(1.14)$

and introducing this into Eq. (1.9), (1.10) we obtain

$$Q=\frac{2EI_s}{lD}\cdot\theta^2\cdot\frac{\left\{-\frac{3}{2}\left(\frac{D}{l}\right)^2+\frac{1}{12}\left(\frac{l}{D}\right)^2\right\}}{\left\{1+\frac{1}{6}\left(\frac{l}{D}\right)^2\right\}}=\frac{2EI_s}{lD}\cdot\theta^2\cdot\beta\,,$$

$\ldots\ldots\ldots(1.15)$

and

$$M=\frac{EI_s}{l}\cdot\theta\cdot\left[1+\frac{\left\{\frac{3}{2}\left(\frac{D}{l}\right)+\frac{1}{3}\left(\frac{l}{D}\right)\right\}}{\left\{1+\frac{1}{6}\left(\frac{l}{D}\right)^2\right\}}\cdot\theta\right]=\frac{EI_s}{l}\cdot\theta\cdot(1+\gamma\theta)\,, \qquad \cdots\cdots\cdots(1.16)$$

in which α, β and γ are factors depending only on the ratio l/D. In Figs. (2), (3) and (4), the values of these factors are plotted against the ratio l/D.

Referring to Fig. (1), we see that the instantaneous center of rotation of the recording pen coincides with the point O where the tangents at the end B_2 and x_2-axis intersect. Then, the geometrical relationship gives

$$\overline{OB_2'}=\frac{Y}{\tan\theta}=\frac{1}{\theta}\left[\frac{l^2}{2EI_s}(-M+PD+Q\delta)\left\{1+\frac{1}{12}\left(\frac{P}{EI_s}\right)l^2\right\}\right.$$
$$\left.-\frac{Ql^3}{6EI_s}\left\{1+\frac{1}{20}\left(\frac{P}{EI_s}\right)l^2\right\}\right]=\frac{l}{2} \quad \text{approximately.}$$

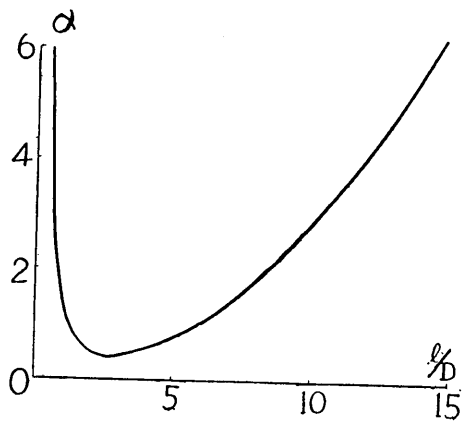

Fig. 2.

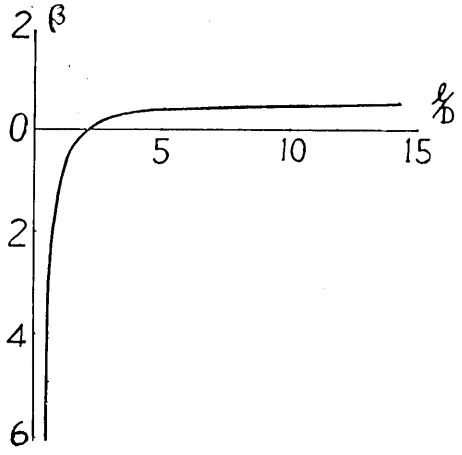

Fig. 3.

Accordingly, the center of rotation of the recording pen remains stationary at the point having the coordinate $x_2=l/2$ and $y_2=0$, i.e., at the mid-point of OB_2'.

In order to determine the validity of these expressions, detailed experiments[7] were carried out, and the experimental results confirmed

7) The results concerning the experiment will be reported in the Journal of the Faculty of Engineering, University of Tokyo, which will be published in the near future.

the validity of these expressions. On comparing these expressions for P, Q and M with the results in the expressions (1.5), we see that, for small value of $l/D(l/D \leqq 1)$, the first approximation differs very little from the second approximation, and that the first approximation differs from the second approximation only by small quantities of second order, so far as the expressions for P and M are concerned.

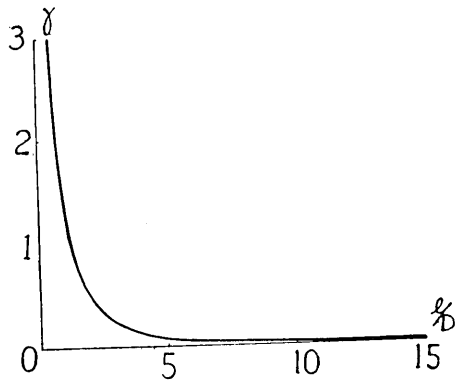

Fig. 4.

Case (2) P_0, Q_0, $M_0 \neq 0$.

In this case, keeping only the first term in the expansions, Eq. (1.1) becomes

$$y_1=\frac{M}{EI_s}\cdot\frac{x_1^2}{2}+\frac{Q}{EI_s}\cdot\frac{x_1^3}{6},$$

$$y_2=\frac{1}{EI_s}\cdot\frac{x_2^2}{6}(-M_0-M+PD-P_0Y+Q_0\delta+Q_0l)$$

$$-\frac{Q_0}{EI_s}\cdot\frac{x_2^3}{2}-\frac{Q}{EI_s}\cdot\frac{x_2^3}{6}.$$

The geometrical relationships (1.5) and (1.8) give

$$\frac{M}{EI_s}l+\frac{Q}{EI_s}\cdot\frac{l^2}{2}=\theta,$$

$$\frac{1}{EI_s}(-M_0l-P_0lY-Ml+PlD+Ql\delta+Q_0l^2)$$

$$-\frac{Q_0}{EI_s}\cdot\frac{l^2}{2}-\frac{Q}{EI_s}\cdot\frac{l^2}{2}=\theta,$$

$$\frac{M}{EI_s}\cdot\frac{l^2}{2}+\frac{Q}{EI_s}\cdot\frac{l^3}{6}-Y=\frac{D}{2}\theta^2,$$

$$Y=\frac{1}{EI_s}\cdot\frac{l^2}{2}(-M_0-M+PD-P_0Y+Q\delta+Q_0l)$$

$$-\frac{Q_0}{EI_s}\cdot\frac{l^3}{6}-\frac{Q}{EI_s}\cdot\frac{l^3}{6}.$$

Solving these equations for P, Q, M and Y algebraically, we obtain the following approximate expressions for P, Q, M and Y:

$$P=\frac{2EI_s}{lD}\left\{1+\frac{3}{2}\left(\frac{D}{l}\right)^2\theta^2\right\}+\frac{M_0}{D}-\frac{Q_0}{2}\cdot\frac{l}{D}\left\{1-\frac{D}{l}\cdot\theta\right\}$$
$$+\frac{P_0Q_0}{D}\cdot\frac{l^3}{24EI_s}+P_0\frac{l}{2D}\theta\left\{1-\frac{1}{2}\left(\frac{D}{l}\right)\theta\right\},$$
$$Q=-\frac{3EI_s}{lD}\cdot\left(\frac{D}{l}\right)^2\cdot\theta^2+\frac{Q_0}{2},$$
$$M=\frac{EI_s}{l}\cdot\theta\cdot\left\{1+\frac{3}{2}\left(\frac{D}{l}\right)\theta\right\}+\frac{Q_0l}{4},$$
$$Y=\frac{l}{2}\theta\left\{1-\frac{1}{2}\left(\frac{D}{l}\right)\theta\right\}+Q_0\frac{l^3}{24EI_s}.$$

For small value of $(D/l)\cdot\theta$, we can neglect the term containing $(D/l)\cdot\theta$ compared with unity. In this way, we obtain the simplified expressions

$$P=\frac{2EI_s}{lD}\theta+\frac{M_0}{D}-\frac{Q_0}{2}\cdot\frac{l}{D}+\frac{P_0Q_0}{D}\cdot\frac{l^3}{24EI_s}+P_0\frac{l}{2D}\theta,$$
$$Q=-\frac{Q_0}{2}-\frac{3EI_s}{lD}\cdot\left(\frac{D}{l}\right)^2\theta^2,$$
$$M=\frac{Q_0}{4}l+\frac{EI_s}{l}\theta,$$
$$Y=\frac{l}{2}\theta+\frac{Q_0l^4}{24EI_s}.$$

In our further discussions, these simplified expressions for P and Y shall be used for the derivation of the equation of motion for the twin strips mechanism.

3. Dynamical Characteristics.

The twin strips have such a wide range of freedom that the rigorous discussion of their dynamical characteristics is a matter of great difficulty. However, from preliminary experiments using a vibration table, it was ascertained that, for an increasing forced frequency, various kinds of resonance, involving a local resonance of strips, occurred successively, and that, under the tacit assumptions that the ratio (l/D)

is relatively small ($l/D<5$) and the center of gravity of the recording pen situated in the vicinity of the center of rotation of the twin strips, the first resonance occurred close to the resonant frequency corresponding to that of the shearing vibration of the twin strips, the mode of which is shown diagrammatically in Fig. 5. Hereafter we will describe this resonant frequency of the shearing vibration as the natural frequency of the twin strips. Accordingly, the working frequency of the twin strips, i.e., the frequency at which the twin strips can be regarded as a perfect magnifying mechanism, should be lower than the natural frequency of the twin strips. From these considerations, when we restrict our discussion to the frequency range smaller than the natural frequency of the twin strips, the following two assumptions may be acceptable: (1) The mass of strips can be neglected, (2) the angle of rotation θ of the recording pen is always proportional to the displacement δ of the movable end ($D\theta=\delta$).

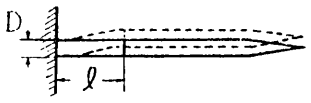

Fig. 5.

Now, in Fig. 6, the general arrangement of the vibrograph with Eden's twin strips is shown schematically. The seismic mass (A) is suspended to the base plate (B) by means of the main springs (C), having the damping apparatus (D). The direction of motion of the seismic mass (A) is restricted to one direction (x-direction) entirely by a suitable guiding device, not shown in the figure. The recording pen (F) attached to the twin strips mechanism (E) gives the trace of vibrations on the recording apparatus (G). The twin strips perform the function as a magnifying mechanism and at the same time produce the additional restoring force, in addition to that of the main springs.

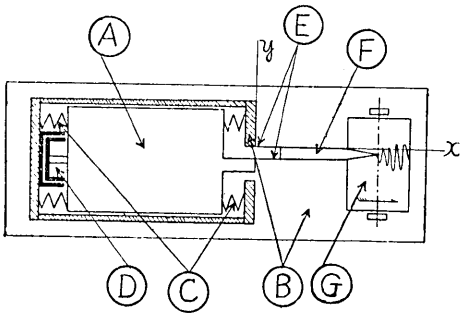

Fig. 6.

Let us take, as shown in Fig. 6, the moving coordinate to be (x, y) fixed to the base plate and assume, for simplicity's sake, that the center of gravity G of the recording pen lies on the tangent at the end B_2 and at a distance r from the end B_2. Then the coordinates of the center of gravity G are

$$x=r\cos\theta, \quad y=l+r\sin\theta+Y.$$

Considering θ and its derivatives with respect to time as small quantities and neglecting terms containing products and powers of small quantities, we obtain

$$\ddot{x}\approx 0, \qquad \ddot{y}\approx r\ddot{\theta}+\ddot{Y}.$$

Let m denote the mass of the recording pen, I the moment of inertia of the recording pen with respect to the center of gravity G, P_0 and Q_0 the component of the reaction force at the end B_2 in x-and y-direction, respectively, M_0 the reaction couple at the same point, P the reaction force at the clamped end A_1 in x-direction, and v_x and v_y the component of the displacement of the forced vibrations in x- and y-direction, respectively. With the arrangement shown in Fig. 6, v_x corresponds to the displacement of the vibration to be measured. Furthermore, let the member B_1B_2 be massless and absolutely rigid, as before. Referring to Fig. 7a, the equations of motion for the recording pen can be written in the form

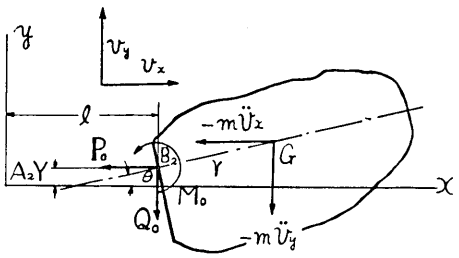

Fig. 7a.

$$m\ddot{x}=-P_0-m\ddot{v}_x=0, \quad \cdots\cdots\cdots\cdots\cdots\cdots \quad (3.1)$$

$$m\ddot{y}=m(r\ddot{\theta}+\ddot{Y})=-Q_0-m\ddot{v}_y, \quad \cdots\cdots\cdots\cdots \quad (3.2)$$

$$I\ddot{\theta}=Q_0r+M_0-P_0r\theta. \quad \cdots\cdots\cdots\cdots\cdots\cdots \quad (3.3)$$

Next, let M denote the mass of the seismic mass, δ its displacement from the equilibrium position, k the spring constant of the main spring, and R the damping constant. Then, referring to Fig. 7c, the equation of motion for the pendulum can be written in the form

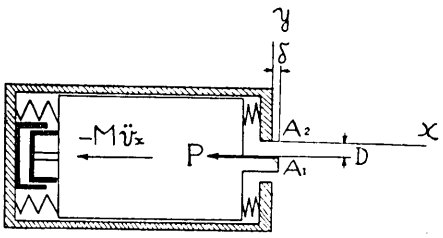

Fig. 7c.

$$M\ddot{\delta}+R\dot{\delta}+k\delta+P=-M\ddot{v}_x.$$

The above assumptions give

$$\delta=D\theta,$$

from which the equation of motion for the pendulum can be reduced to

$$MD\ddot{\theta}+RD\dot{\theta}+kD\theta+P=-M\ddot{v}_x. \quad \cdots\cdots\cdots\cdots \quad (3.4)$$

Referring to Fig. 7b, as derived above, the approximate expressions for P and Y are

$$P=\frac{2EI_s}{lD}\theta+\frac{M_0}{D}-\frac{Q_0 l}{2D}+P_0Q_0\frac{l^3}{24EI_s}$$
$$+P_0\frac{l}{2D}\theta\,, \quad \cdots\cdots\cdots\cdots \quad (3.5)$$

$$Y=\frac{l}{2}\theta+Q_0\frac{l^3}{24EI_s}\,. \quad \cdots\cdots\cdots\cdots \quad (3.6)$$

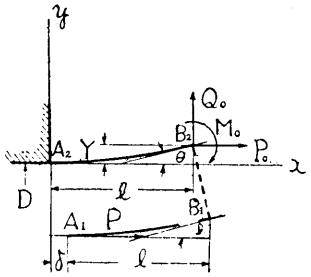

Fig. 7b.

Eliminating P, P_0, Q_0, and M_0 from the equations (3.1), (3.2), (3.3), (3.4), and the expression (3.5), and using the notations

$L=l/2+r$=distance between the center of gravity G and the center of rotation O,

$K=k+2EI_s/(lD^2)$=effective spring constant,

we, after neglecting $\frac{ml^2}{12EI_s}\cdot\ddot{v}_x$ and $\frac{mL}{KD^2}\ddot{v}_y$ compared with unity, obtain

$$\ddot{\theta}\left(MD+\frac{I}{D}+\frac{m}{D}rL\right)+RD\dot{\theta}+\ddot{Y}\frac{m}{D}L+KD\theta=-M\ddot{v}_x-\ddot{v}_y\frac{m}{D}L. \quad (3.7)$$

Eliminating Q_0 from the equation (3.2) and the expression (3.6), we obtain

$$Y=\frac{l}{2}\theta-\frac{ml^3}{24EI_s}\cdot\ddot{v}_y-\frac{ml^3}{24EI_s}r\ddot{\theta}-\frac{ml^3}{24EI_s}\ddot{Y}. \quad \cdots\cdots\cdots \quad (3.8)$$

Eliminating Y and its derivatives with respect to time t from the equation (3.7) and the expression (3.8), and using the notations

$$M_0=M+\frac{I}{D^2}\,, \quad M_e=M_0+m\frac{L^2}{D^2}\,, \quad \rho=\frac{ml^3}{24EI_s}\,,$$

we obtain

$$M_0\dddot{\theta}+R\ddot{\theta}+\ddot{\theta}\left(K+\frac{M_e}{\rho}\right)+\frac{R}{\rho}\dot{\theta}+\frac{K}{\rho}\theta=-\frac{M}{D}\dddot{v}_x-\frac{M}{D\rho}\ddot{v}_x-\frac{m}{D^2}\cdot\frac{L}{\rho}\cdot\ddot{v}_y\,. \quad (3.9)$$

Eliminating θ and its derivatives with respect to time t from the equation (3.7) and the expression (3.8) and neglecting $\frac{\rho}{K}\cdot\frac{mL}{D^2}\cdot\dddot{v}_y$ compared with unity, we obtain

$$M_0\dddot{Y}+R\ddot{Y}+\dot{Y}\left(K+\frac{M_e}{\rho}\right)+\frac{R}{\rho}\dot{Y}+\frac{K}{\rho}Y=-\frac{M}{\rho}\cdot\frac{l}{2D}\cdot\ddot{v}_x$$
$$+\frac{M}{D}r\cdot\ddddot{v}_x-\left(M_0+\frac{mLr}{D^2}\right)\dddot{v}_y-R\ddot{v}_y-K\left(1+\frac{m}{K\rho}\cdot\frac{Ll}{D^2}\right)\cdot\dot{v}_y. \quad .. \quad (3.10)$$

Thus, after disregarding all non-linearities, we obtain these two linear differential equations from which the dynamical characteristics has to be determined. In analysing these differential equations, it is convenient to distinguish between an acceleration seismograph (accelerograph) and a displacement seismograph (vibrograph). In a displacement seismograph, on account of its low natural frequency, the restoring force is usually limited to within a relatively low limit. Therefore, the additional restoring force of the twin strips also must be small, and this requirement is not consistent with the demand for a wide working frequency range of the twin strips. In an acceleration seismograph, on the other hand, its considerably high natural frequency enables the twin strips to perform their proper function up to the maximum frequency which can be measured without difficulty.

Case (1) Displacement-Seismograph

Now we will consider the forced vibration only and disregard the transient free vibrations and assume that the forced vibration is a harmonic vibration with circular frequency ω. Then we can put

$$v_x=V_xe^{j\omega t},$$
$$v_y=V_ye^{j\omega t},$$
$$\theta=\theta_me^{j\alpha}e^{j\omega t}=\Theta e^{j\omega t},$$
$$y=y_me^{j\beta}e^{j\omega t}=\mathfrak{Y}e^{j\omega t},$$

where α and β are a phase angle, Θ and $\mathfrak{Y}$ being generally complex numbers.

Introducing these expressions and their derivatives with respect to time into the equations (3.9) and (3.10) and introducing the notations

$f^*=\frac{1}{2\pi}\sqrt{\frac{K}{M_e}}$=natural frequency of the pendulum,

$f_0=\frac{1}{2\pi}\sqrt{\frac{24EI_s}{ml^3}}=\frac{1}{2\pi}\sqrt{\frac{1}{\rho}}$=natural frequency of the twin strips,

$f=\omega/2\pi$=frequency of the forced vibration,

$u=f^*/f$=frequency ratio,

$\mu = f/f_0$ = frequency ratio,

and

$$h = \frac{R}{2\sqrt{M_e K}} = \text{damping constant},$$

we obtain

$$\mathfrak{Y} = \frac{\frac{M}{M_e}\cdot\frac{l}{2D}\cdot V_x\cdot\left(1-\frac{2r}{l}\mu^2\right)}{\left\{(1-\mu^2)(u^2-1+j2hu)-\mu^2\left(\frac{M_e-M_0}{M_0}\right)\right\}} - \rho V_y\omega^2\cdot\frac{\left[\left\{1+\frac{m}{M_e}\cdot\frac{L}{D^2}\cdot(r-L)\right\}+j2hu+u^2\left(1+\frac{m}{\rho K}\cdot\frac{lL}{2D^2}\right)\right]}{\left\{(1-\mu^2)(u^2-1+j2hu)-\mu^2\left(\frac{M_e-M_0}{M_0}\right)\right\}}, \quad \cdots\cdots\cdots (3.11)$$

$$\Theta = \frac{\frac{M}{M_e}\cdot\frac{1}{D}\cdot V_x(1-\mu^2)}{\left\{(1-\mu^2)(u^2-1+j2hu)-\mu^2\left(\frac{M_e-M_0}{M_0}\right)\right\}} - \frac{\frac{m}{M_e}\cdot\frac{L}{D^2}\cdot V_y}{\left\{(1-\mu^2)(u^2-1+j2hu)-\mu^2\left(\frac{M_e-M_0}{M_0}\right)\right\}}. \quad \cdots\cdots (3.12)$$

From these expressions, the amplitude Θ and $\mathfrak{Y}$ of the forced vibration can be calculated for any value of μ or u. In a displacement seismograph, it is essential that the natural frequency f^* of the pendulum should be lower (slower) than the minimum frequency to be measured and the natural frequency f_0 of the twin strips higher than the maximum frequency to be measured. The natural frequency f_0 of the twin strips, therefore, should be very much higher than the natural frequency f^* of the pendulum and μ, for low frequency near or lower than the natural frequency $f^*(u \geqq 1)$, can be considered as small quantity. Consequently, the expressions (3.11), (3.12), for small values of $\frac{M_e-M_0}{M_0}$ and $\frac{2r}{l}$ which we usually have, can be expressed in the approximate form

$$\mathfrak{Y}=\frac{-\frac{M}{M_e}\cdot\frac{l}{2D}V_x}{(u^2-1+j2hu)}-\rho V_y\omega^2\cdot\frac{\left[\left\{1+\frac{m}{M_e}\cdot\frac{L}{D^2}(r-L)\right\}+j2hu+u^2\left(1+\frac{m}{\rho K}\cdot\frac{Ll}{2D^2}\right)\right]}{(u^2-1+j2hu)}, \quad \cdots\cdots\cdots (3.13)$$

$$\Theta=\frac{-\frac{M}{M_e}\cdot\frac{1}{D}V_x}{(u^2-1+j2hu)}+\frac{-\frac{m}{M_e}\cdot\frac{L}{D^2}\cdot V_y}{(u^2-1+j2hu)}. \quad \cdots\cdots\cdots\cdots\cdots (3.14)$$

The second terms of these equations represent the undesirable displacement for which the transverse component V_y of the forced vibration is responsible. In order to perform the proper function as a magnifying mechanism, it is neccessary that these undesirable terms should be made negligible compared with the first terms. Fortunately, in most cases, these terms can be made negligible by proper dimensioning. When these requirements are fulfilled, the first terms indicate that the twin strips can be regarded as a perfect magnifying mechanism, i.e., the recording pen rotates about the point O having the coordinates $x=\frac{l}{2}$ and $y=O$ and its short arm is equal to D.

Next, for the frequency range above the natural frequency f^* of the pendulum, i.e., for the working frequency-range of a displacement seismograph ($u<1$), it is well known that

$$(u^2-1+j2h)\approx -1.$$

For such frequency range, introducing the new notations

$$a=\frac{\left(1-\frac{2r}{l}\mu^2\right)}{\left(1-\mu^2\cdot\frac{M_0}{M_e}\right)}, \qquad b=\frac{(1-\mu^2)}{\left(1-\mu^2\cdot\frac{M_0}{M_e}\right)},$$

Eq. (3.11) can be expressed in the approximate form

$$\mathfrak{Y}=-\frac{M}{M_e}\cdot\frac{l}{2D}\cdot V_x\cdot a-\rho\omega^2 V_y\cdot\frac{\left\{1+\frac{m}{M_e}\cdot\frac{L}{D^2}\cdot(r-L)+u^2\frac{m}{\rho K}\cdot\frac{Ll}{2D^2}\right\}}{\left(1-\mu^2\frac{M_0}{M_e}\right)}, \quad \cdots\cdots\cdots (3.15)$$

$$\Theta=-\frac{M}{M_e}\cdot\frac{1}{D}\cdot V_x\cdot b-\frac{m}{M_e}\cdot\frac{L}{D^2}\cdot\frac{1}{\left(1-\mu^2\dfrac{M_0}{M_e}\right)}\cdot \quad \cdots\cdots\cdots\cdots \quad (3.16)$$

When the second terms of these equations can be made negligible compared with the first terms, as before, the first terms define the dynamical characteristics of the twin strips. In Fig. 8, the values of the magnification factor b for various values of M_0/M_e are plotted against the frequency ratio μ, and in Fig. 9, the values of the magnification factor

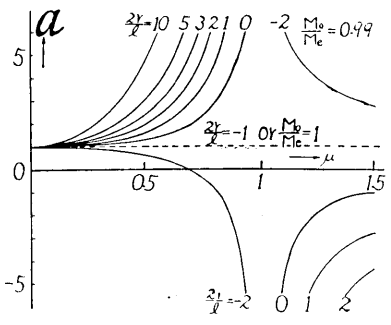

Fig. 8.

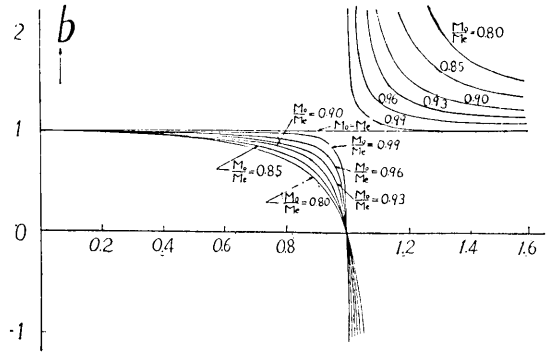

Fig. 9.

a for various values of $2r/l$ are plotted against the frequency ratio μ for a particular case in which $M_0/M_e=0.99$.

In a optical record, the recorded magnitude depends only upon Θ, i.e., for the frequencies at which the magnification factor b differs only slightly from unity, the twin strips can perform their proper function.

In mechanical records, the recorded magnitude depends upon Θ as well as $\mathfrak{Y}$. Referring to Fig. 10, the displacement of the tip of the recording pen of length l_0 becomes

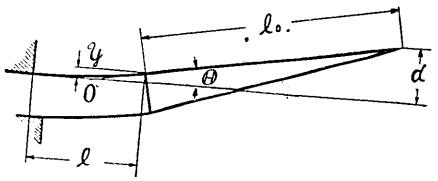

Fig. 10.

$$d=\mathfrak{Y}+\Theta\cdot l_0\cdot=\frac{M_0}{M_e}\cdot\frac{V_x}{D}\cdot\left(l_0+\frac{l}{2}\right)\cdot c, \quad \cdots\cdots\cdots \quad (3.17)$$

in which

$$c=\left\{1-\mu^2\cdot\frac{l_0-r}{l_0+l/2}\right\}\Big/\left\{1-\mu^2\cdot\frac{M_0}{M_e}\right\}. \quad \cdots\cdots\cdots \quad (3.18)$$

In this case, for the frequencies at which the magnification factor

c differs only slightly from unity, the twin strips can be regarded as a complete magnifying mechanism, in which the effective length of the recording pen is $(l/2+l_0)$ and the short arm D.

In Fig. 11, the values of the magnification factor c for various values of $(2r/l)$ are plotted against the frequency ratio μ for a particular case in which $l_0=10$ cm, $l=1$ cm, and $M_0/M_e=0.99$. The dotted line corresponds to the particular case in which $M_0/M_e=1$ or $2r/l=-1(L=0)$.

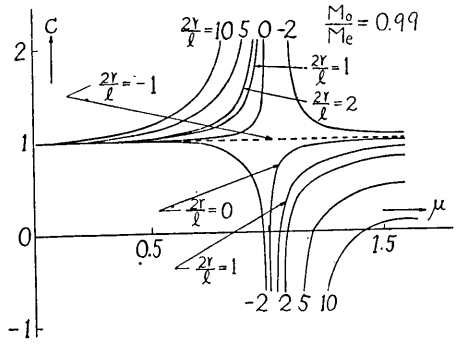

Fig. 11.

By proper dimensioning, we can improve the dynamical characteristics. Now, if we put $L=0$ or $2r/1=-1$, the expression (3.15), (3.16) can be expressed in the more simplified form

$$\Theta=-\frac{M}{M_e}\cdot\frac{1}{D}\cdot V_x, \quad \cdots\cdots\cdots\cdots\cdots\cdots \quad (3.19)$$

$$\mathfrak{Y}=-\frac{M}{M_e}\cdot\frac{l}{2D}\cdot V_x-\frac{\rho\omega^2 V_y}{(1-\mu^2)}. \quad \cdots\cdots\cdots\cdots \quad (3.20)$$

In this case, if the transverse component V_y of the forced vibration vanishes, the magnification of the twin strips may be independent of the forced frequency f. The undesirable second term, however, becomes extremely large as the forced frequency f approaches the natural frequency f_0 of the twin strips ($\mu\approx1$). Therefore the maximum working frequency of the twin strips should be lower than the natural frequency f_0 of the twin strips, but in most cases can be extended to $0.9\,f_0$. Thus, in order to expand the working frequency range of the twin strips, it is effective to make L as small as practicable.

The magnitude of this undesirable term is equivalent to the displacement of the recording pen for a particular case in which the seismic mass is rigidly clamped to the base plate in its equilibrium position, and can be determined experimentally by the use of a vibration table.

Case (2) Acceleration Seismograph

In a acceleration seismograph, after rearranging, the expressions (3.11), (3.12) can be reduced to

$$\mathfrak{Y}=\frac{\omega^2 V_x}{(2\pi f^*)^2}\cdot\frac{M}{M_e}\cdot\frac{l}{2D}\cdot\frac{\left(1-\frac{2r}{l}\mu^2\right)}{\left\{(1-\mu^2)\left(1-\frac{1}{u^2}+j\frac{2h}{u}\right)-\frac{\mu^2}{u^2}\left(\frac{M_e-M_0}{M_0}\right)\right\}}$$

$$+\rho V_y\omega^2\cdot\frac{\left[\left(1+\frac{m}{\rho K}\cdot\frac{Ll}{2D^2}\right)-\frac{1}{u^2}\left\{1+\frac{m}{M_e}\cdot\frac{L}{D^2}(r-L)\right\}+j\frac{2h}{u}\right]}{\left\{(1-\mu^2)\left(1-\frac{1}{u^2}+j\frac{2h}{u}\right)-\frac{\mu^2}{u^2}\left(\frac{M_e-M_0}{M_0}\right)\right\}}, \quad (3.21)$$

$$\Theta=\frac{\omega^2 V_x}{(2\pi f^*)^2}\cdot\frac{M}{M_e}\cdot\frac{1}{D}\cdot\frac{(1-\mu^2)}{\left\{(1-\mu^2)\left(1-\frac{1}{u^2}+j\frac{2h}{u}\right)-\frac{\mu^2}{u^1}\left(\frac{M_e-M_0}{M_0}\right)\right\}}$$

$$+\frac{\omega^2 V_y}{(2\pi f^*)^2}\cdot\frac{m}{M_e}\cdot\frac{L}{D^2}\cdot\frac{1}{\left\{(1-\mu^2)\left(1-\frac{1}{u^2}+j\frac{2h}{u}\right)-\frac{\mu^2}{u^2}\left(\frac{M_e-M_0}{M_0}\right)\right\}}\cdot$$

..... (3.22)

Now, it is desirable that the natural frequency f_0 of the twin strips should be at least several times larger than the natural frequency f^* of the pendulum, and this, on account of high natural frequency of an acceleration seismograph, is always possible. As is well known, for the working frequency of an acceleration seismograph the value of $(1-1/u^2+j2h/u)$ differs only slightly from unity and this occurs when the frequency to be measured is low as compared with the natural frequency f^* of the pendulum. Then, for such frequency range (working frequency range), $1/u^2$ and μ^2 can be neglected compared with unity. Consequently, the expressions (3.21), (3.22) can be expressed in the approximate form

$$\mathfrak{Y}=\frac{\omega^2 V_x}{(2\pi f^*)^2}\cdot\frac{M}{M_e}\cdot\frac{l}{2D}+\rho\omega^2 V_y\left(1-\frac{m}{\rho K}\cdot\frac{Ll}{2D^2}\right), \quad .... (3.23)$$

$$\Theta=\frac{\omega^2 V_x}{(2\pi f^*)}\cdot\frac{M}{M_e}\cdot\frac{1}{D}+\frac{\omega^2 V_y}{(2\pi f^*)^2}\cdot\frac{m}{M_e}\cdot\frac{L}{D^2}\cdot \quad ..... (3.24)$$

When the second terms of these equation can be neglected compared with the first terms, as before, the first term indicates that the twin strips can perform their proper function. Moreover, if we put $L=0$ or $2r/l=-1$, these expressions can be expressed in the more simplified form

$$\mathfrak{Y}=\frac{\omega^2 V_x}{(2\pi f^*)^2}\cdot\frac{M}{M_e}\cdot\frac{l}{2D}+\rho\omega^2 V_y, \quad ..... (3.25)$$

$$\theta = \frac{\omega^2 V_x}{(2\pi f^*)} \cdot \frac{M}{M_e} \cdot \frac{1}{D} . \quad \cdots\cdots\cdots\cdots\cdots\cdots \quad (3.26)$$

Thus, in an acceleration seismograph, we need only make the natural frequency f_0 of the twin strips at least several times larger than the natural frequency f^* of the pendulum, which is always possible.

Experiment:

1) Vibration table:

We investigated the foregoing theory by an experiment using a vibration table, of which the constructional details are given in Figs. 12

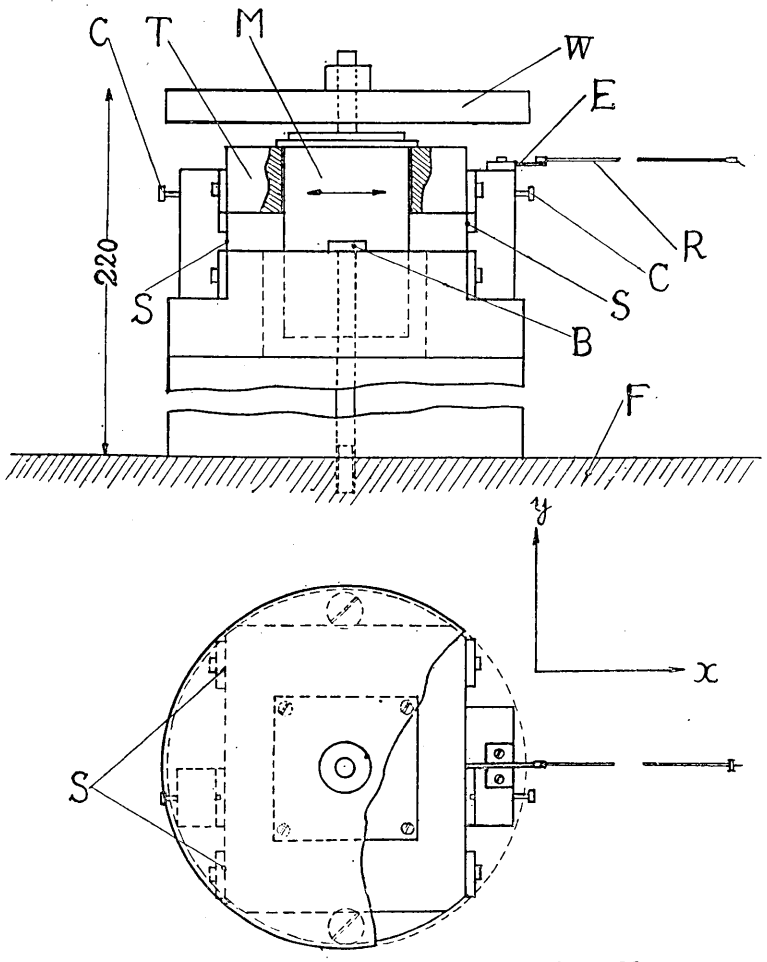

Fig. 12. Constructional details of vibration table.

and 13. The purposely unbalanced fly-wheel W of aluminum-alloy, 15 cm. in diameter and 810 g. in weight, is directly coupled to an axle of a small D.C. motor M fed by 24 V. battery. This motor is firmly bolted to a rigid table T of aluminum-alloy, 12 cm. wide by 10 cm. long by 3 cm. thick. A table T is held between two pairs of flat paralled phosphor-bronze strips S. Eacn strip is 0.025 cm. thick by 0.5 cm. wide by 1.5 cm. long. By means of this simple flat strips suspension the direction of motion of the seismic element is restricted to the x-direction entirely without friction, but some reduction in lateral (y-direction) and torsional stability of the suspension may be involved. However, no appreciable instability (shimmering) was observed concerning this experiment. The natural frequency of the suspension was found to be about 4 c/s. The recording pen R is attached to Eden's twin strips E to be tested, and the movement of the tip of the recording pen is recorded on smoked paper wound upon a drum driven by Warren synchronous motor (6 W). Damping is not intentionally provided ($h=0$), but moderate damping is desirable to reduce the free vibration caused by external vibrations. The seismic element may be clamped by a clamping screw C. The base plate P of alluminum-alloy is rigidly bolted to a massive foundation F of cast-iron by means of two long bolts B. The vibrational frequency of the vibration table can be controlled by varying the rotational speed of a motor M, and the vibrational frequency available in our experiments were of the range 2 c/s to 80 c/s.

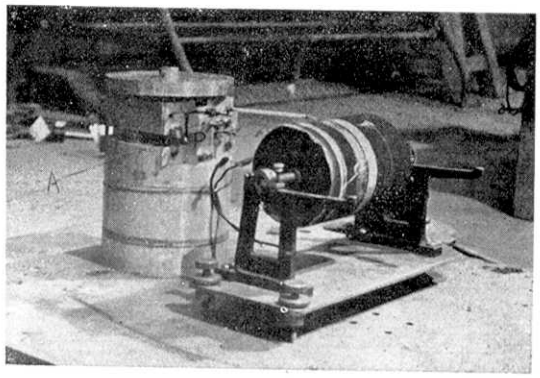

Fig. 13. General view of vibration table.

2) Experiment method and results:

The twin strips used in these experiments were constructed of a main spring of a wrist watch (special steel) by soldering, and had the following dimensions: Length l, 1.9 cm.: width, 0.14 cm.: thickness, 0.009 cm.; distance between both strips D, 0.38 cm.: length ratio l/D, 5. The recording pen was of straw, and its full length l_0 was 10 cm. The magnification of the movements of the seimic element at the tip of the recording pen was about 26 times. Although the experiments were

made for various values of $2r/l$ as shown in Table I, the mass m of the recording pen was kept constant ($m=3.5$ g.) throughout the experiments, and hence the natural frequency f_0 of the twin strips, defined by the formula

$$f_0=\frac{1}{2\pi}\cdot\sqrt{\frac{24EI_s}{ml^3}}\ ,$$

was also kept constant ($f_0=19$ c/s).

Table I.

Case	I	II	III	IV
$2r/l$	+2.1	−0.02	−0.40	−0.65
M_0/M_e	0.99	0.99	0.99	0.99

The original data recorded on smoked papers were generally of the type shown in Fig. 14, which corresponds to Case I.

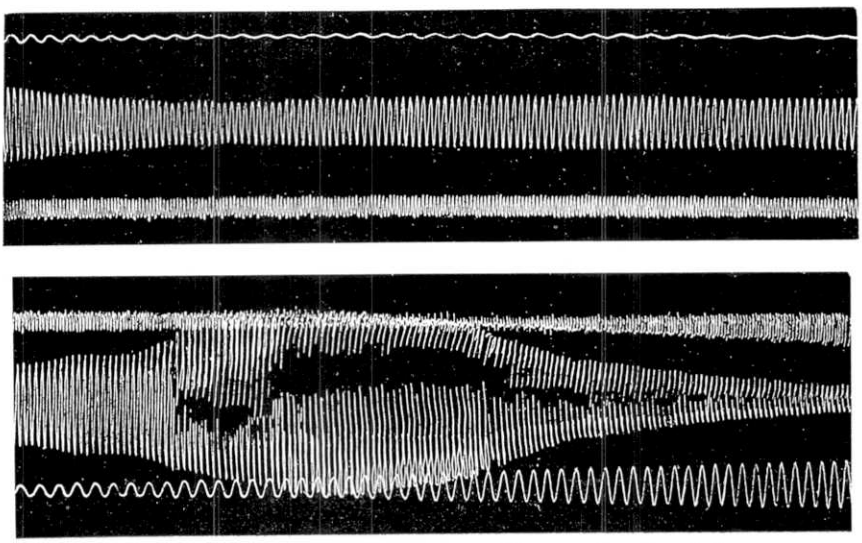

Fig. 14. Forced vibration of Case I at different vibrational frequency.

With the vibration table just mentioned, the expression (3.17), obtained previously for a displacement seismograph, may be readily reduced to

$$d=\mathfrak{Y}+\Theta l_0=\frac{\overline{mr}}{\left(M+\frac{I}{D^2}+m\frac{L^2}{D^2}\right)}\cdot\frac{\left(l_0+\frac{l}{2}\right)}{D}\cdot\frac{1-\left(\frac{f}{f_0}\right)^2\cdot\frac{l_0-r}{\left(l_0+\frac{l}{2}\right)}}{1-\left(\frac{f}{f_0}\right)^2\cdot\frac{\left(M+\frac{I}{D^2}\right)}{\left(M+\frac{I}{D^2}+m\frac{L^2}{D^2}\right)}},$$

$$\mu=f/f_0, \qquad L=l/2+r,$$

in which $\overline{mr}$ denotes the unbalanced moment of the fly-wheel, M the total mass of the seismic element (the table T, a motor M, and the fly-wheel F together), and the other symbols have the same meanings as before. This equation holds, of course, only when the vibrational frequency f is much higher than the natural frequency f^* of the vibration table (suspension). In Figs. 15~18, the absolute values of d calculated from this equation for various values of $2r/l$ are shown by

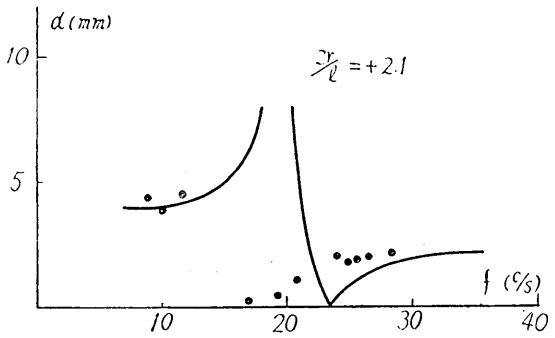

Fig. 15

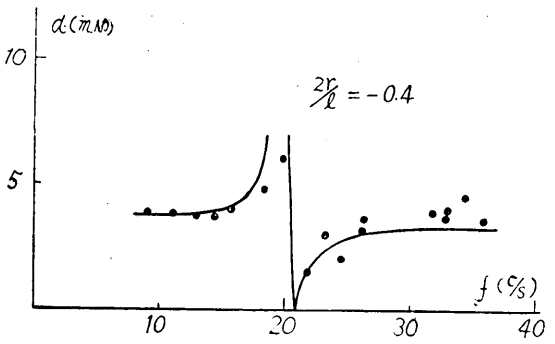

Fig. 16

full lines, while the plottings show the value obtained by experiments.

From Figs. 15~18, it will be seen that the two values, theoretical and experimental, are in fair accord, particularly at the working frequency range of the twin strips.

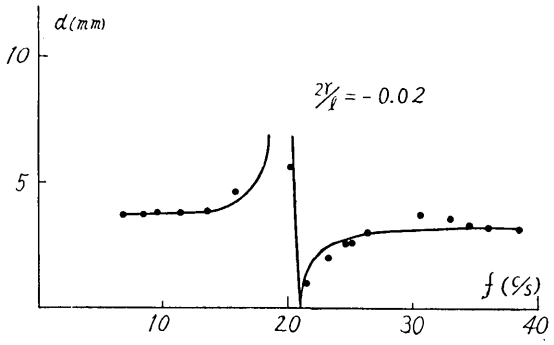

Fig. 17.

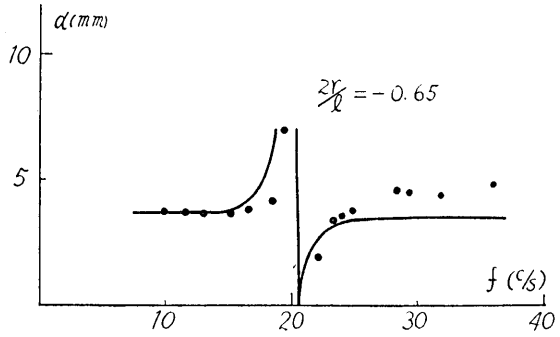

Fig. 18.

Finally, comparison was made between the seismogram of ordinary seismograph and that of the seismograph with twin strips. These two seismographs were installed at the same place (Earthquake Research

Table II. Instrumental Constants of the Seismographs

Constants / Kinds	Natural Period (sec)	Magnification	Damping ratio
Seismograph with Eden's twin strips	1.0	110	13:1
Seismograph with commonly used magnifying mechanism	1.0	98	10:1

Institute), and had nearly the same instrumental constants as shown in Table II.

The commonly used magnifying mechanism of ordinary inverted pendulum seismograph was replaced by Eden's twin strips mechanism as shown in Figs. 19 and 20, and the supporting spring and twin strips were designed so as to make the natural frequency and the magnification nearly equal to those of the seismograph to be compared.

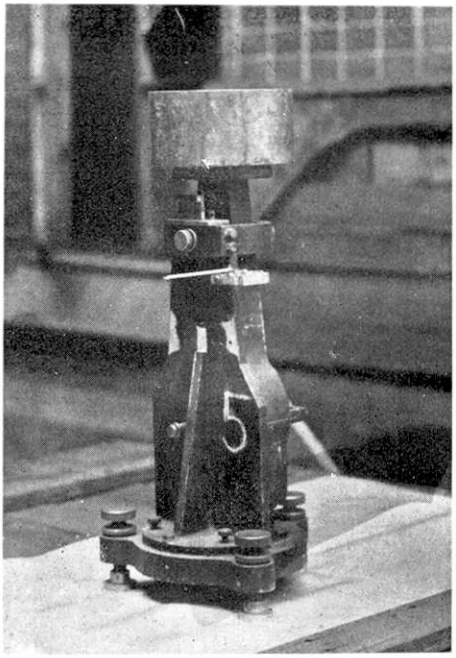

Fig. 19. Inverted Pendulum Seismograph with Eden's Twin Strips Composed of X-ray Photographic Film.

Eden's twin strips attached to this seismograph were of x-ray photographic film in order to minimize the additional restoring force of twin strips, and had the following dimensions: Length l, 1.4 cm.: width, 0.2 cm.: thickness, 0.02 cm.: distance between both strips D, 0.1 cm.: length ratio l/D, 14. The theoretically assumed maximum working frequency of twin strips was about 30 c/s.

In Figs. 21a and 21b, the typical seismograms are shown which were caused by the earthquake of December 7, 1953. Fig. 21a cor-

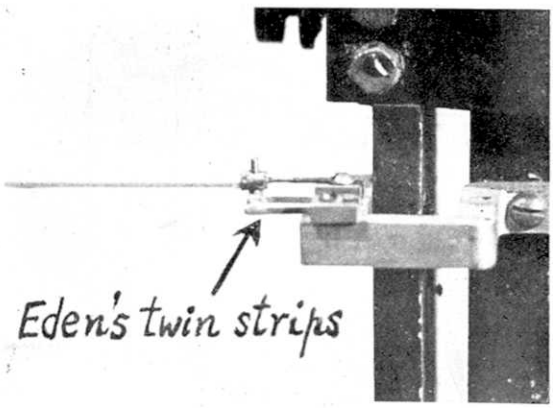

Fig. 20. Enlarged view of Eden's twin strips of the seismograph shown in Fig. 19.

responds to the seismogram of the ordinary seismograph, while Fig. 21b to that of the seismograph with Eden's twin strips composed of X-ray photograpic film. From many seismograms thus obtained, it was ascertained that these seismograms agree closely with each other.

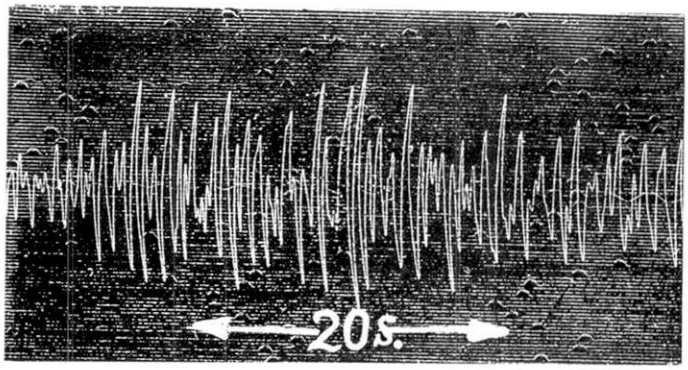

Fig. 21a.

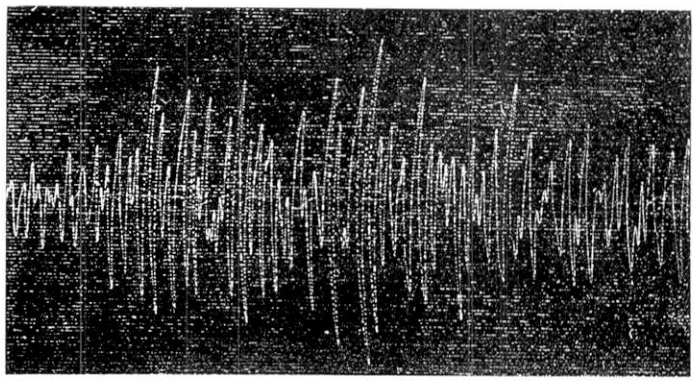

Fig. 21b.

Seismograms recording the earthquake of Dec. 7, 23 h., 12 m., 1953.
Fig. 21a: ordinary seismograph.
Fig. 21b: seismograph with Eden's twin strips.

7. エデン平行薄片の理論と地震計への応用

地震研究所 西村源六郎
鈴木正治
中央大学工学部 古川英一

Eden の twin strips は Millionth の Comparator に用いられている静的拡大機構である．これに関する理論は発表されていない．又その特性の実験的研究もみあたらない．

本研究では Eden の twin strips の静的特性と動特性を理論的に研究し，これが地震計に応用して充分に使用し得る事を述べ，かつ現在用いられている地震計の拡大機構にみられる欠点即ち機構の複雑性，部品間にあるがたや摩擦，製作の容易でない事，かさばる事，製作費のかさむ事その他の欠点を Eden の twin strips を用いる事によつて充分に除却し得る事を述べてある．又簡単に高倍率の地震計も求める事が出来るのであつて，これによる高倍率地震計を製作中である事を述べておく．

尚振動工学方面へ Eden の twin strips を用いた研究に関しては5年位前から著者達によつて行われて来ていて，可なり見るべき研究結果を得ている．例えば，家庭用ミシンの反動力の測定，工作機械特に grinder の加工時の振動研究，又噛合時に於ける歯車の噛合誤差に関する研究，電蓄 record の針先摩擦についての測定，ミシンの始動トルクの測定，その他 focal plane shutter 写真機の torsional moment の測定，或いは shutter の速度特性の研究等に応用している．これ等に関する報告は東京大学工学部記要，精機学会誌等の最近のものに発表し又近い内に出版されるものである．